Molecular Crystals and Liquid Crystals
Publication details, including instructions for authors and subscription information:
http://www.tandfonline.com/loi/gmcl16

Angular Dependence of the Acousto-Optical Effect

Charles F. Hayes [a]

[a] Department of Physics and Astronomy, University of Hawaii, Honolulu, Hawaii, 96822

Version of record first published: 14 Oct 2011.

To cite this article: Charles F. Hayes (1981): Angular Dependence of the Acousto-Optical Effect, Molecular Crystals and Liquid Crystals, 75:1, 69-86

To link to this article: http://dx.doi.org/10.1080/00268948108073604

Mol. Cryst. Liq. Cryst., 1981, Vol. 75, pp. 69–86
0026-8941/81/7504–0069 $06.50/0

Printed in the United States of America

Angular Dependence of the Acousto-Optical Effect

CHARLES F. HAYES

Department of Physics and Astronomy, University of Hawaii, Honolulu, Hawaii 96822

(*Received November 25, 1980*)

Equations are derived giving the transmission as a function of incident angle for ultrasonic waves passing through a liquid crystal cell. These equations are tested experimentally and compared with the light transmission which occurs via the "acousto-optic effect." Maximum light transmission is found to occur for angles of maximum ultrasonic transmission. It would appear the equations can be used to prescribe cell design for maximizing the effect for a given ultrasonic frequency.

I INTRODUCTION

Normally no light is transmitted if a homeotropically aligned nematic liquid crystal cell is placed between crossed polarizers. However, light is transmitted if an ultrasonic wave is directed to the cell. Since 1976 it has been known[1] that the mechanism responsible for the effect is acoustic streaming. However, the dependence of the transmitted light intensity upon the incident ultrasonic angle is not understood. In 1978, Letcher, Lebrun, and Candau[2] reported for their cells the effect took place in a relatively narrow range of incident angles, 27 to 30 degrees. In 1977, Nagai, Peters and Candau[3] and, in 1978, Nagai and Iizuka[4] reported the transmitted light intensity as a function of ultrasonic frequency and incident angle. Their results indicated the transmitted light intensity increased with increased ultrasonic transmission through the cell. In 1979, Perbet, Hareng, and LeBerre[4] reported strong light transmission at incident ultrasonic angles of maximum *and minimum* ultrasonic transmission. Also, in 1979, Lebrun, Candau, and Letcher[6] reported the narrow angular range for the effect becomes broadened if very thin glass is used for the cell walls.

In this report we describe the study we have undertaken to analyze the angular dependence of this effect. In Section II a theory is developed which gives the ultrasonic transmission of the cell as a function of: incident ultrasonic angle, ultrasonic frequency, speed of the ultrasonic wave in the fluid(s) surrounding the cell, density of the liquid crystal, density of the fluid(s) surrounding the

cell, density of the cell walls, speeds of the longitudinal and transverse waves in the glass, thickness of the cell walls, thickness of the liquid crystal and ultrasonic speed in the liquid crystal. Since each of these quantities are measurable, as well as the actual transmission, the final equation can rigorously be tested experimentally. The results of such testing is reported in Section III. A comparison is also made in this section between ultrasonic transmission and sensitivity to the effect. This comparison gives insight into the results mentioned above by other researchers. We also obtain results for the angular dependence of striations which often appear in the cells. In the final sections conclusions are drawn from these observations.

II THEORY

To obtain an expression for the transmission of an acoustic wave through a liquid crystal cell, we will use the coordinate system of Figure 1. Although experimentally we will immerse the cell in water the expression will allow the fluid on each side of the cell to be different.

Since fluids support no shear waves we will only have one wave function in the water and liquid crystal regions, a wave function for the compression wave:

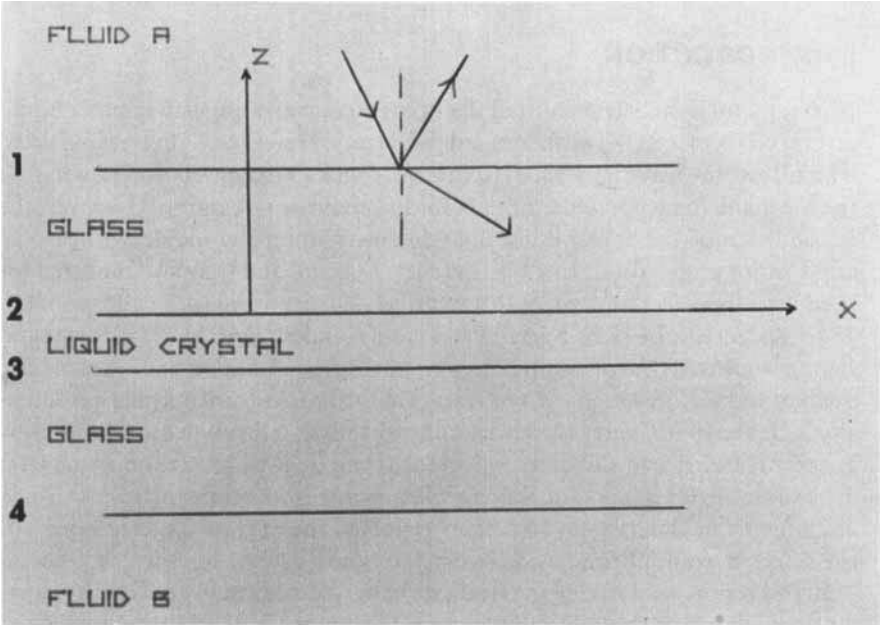

FIGURE 1 Gives the coordinate system for the liquid crystal cell. The origin is at the first glass-liquid crystal interface for the initial matrix calculation and is moved for the final matrix calculation to the lower glass-fluid *B* interface.

$$\phi = (\phi' e^{i\alpha z} + \phi'' e^{-i\alpha z}) e^{i(\sigma x - \omega t)} \tag{1}$$

In the glass we will have an additional function for shear:

$$\Psi = (\Psi' e^{i\beta z} + \Psi'' e^{-i\beta z}) e^{i(\sigma x - \omega t)} \tag{2}$$

We note that the x component of the wave number, σ, is the same for both types of waves. Due to Snell's law we further see σ is the same in each medium.

The material speeds may be found from

$$v_x = \frac{\partial \phi}{\partial x} - \frac{\partial \Psi}{\partial z} \tag{3}$$

and

$$v_y = \frac{\partial \phi}{\partial x} + \frac{\partial \Psi}{\partial z} \tag{4}$$

The wave speeds may be expressed in terms of the Lame' parameters (λ, μ) and the density, ρ. The longitudinal speed is given by

$$c = \sqrt{\frac{\lambda + 2\mu}{\rho}} \tag{5}$$

and the shear speed by

$$b = \sqrt{\frac{\mu}{\rho}} \tag{6}$$

For the fluid region the only stress is the pressure, since $\mu = 0$, but for the glass regions we must generalize to

$$z_z = \lambda \left(\frac{\partial u}{\partial x} x + \frac{\partial u}{\partial z} z \right) + 2\mu \frac{\partial u}{\partial x} z \tag{7}$$

$$z_x = \mu \left(\frac{\partial u_x}{\partial z} + \frac{\partial u_z}{\partial x} \right) \tag{8}$$

where u_x and u_z are material displacements from equilibrium in the x and z directions, respectively. These displacement components are related to the speed components by

$$u_x = \frac{iv}{\omega} x \tag{9}$$

$$u_z = \frac{iv}{\omega} z \tag{10}$$

As indicated in Figure 1 we use the subscript 1 to denote the water glass interface at $z = d$. We let

$$P = \alpha d = \omega d \cos \theta / c \text{ and } Q = \beta d = d \cos \gamma / b$$

Combining Eqs. 1-4 and 7-10 we have

$$\begin{pmatrix} v_{x_1} \\ v_{z_1} \\ z_{z_1} \\ \frac{1}{2\mu} z_{x_1} \end{pmatrix} = A \begin{pmatrix} \phi' + \phi'' \\ \phi' - \phi'' \\ \Psi' - \Psi'' \\ \Psi' + \Psi'' \end{pmatrix} \tag{11}$$

where

$$A = \begin{pmatrix} i\sigma \cos P & -\alpha \sin P \\ -\alpha \sin P & i\alpha \cos P \\ -\frac{i}{\omega}(\lambda k^2 + 2\mu\alpha^2) \cos P & \frac{1}{\omega}(\lambda k^2 + 2\mu\alpha^2) \sin P \\ \frac{\alpha\sigma}{\omega} \sin P & \frac{-i\alpha\sigma}{\omega} \cos P \end{pmatrix}$$

$$\begin{pmatrix} -i\beta \cos Q & \beta \sin Q \\ -\sigma \sin Q & i\sigma \cos Q \\ \frac{-2i\mu\sigma}{\omega} \beta \cos Q & \frac{2\mu\sigma\beta}{\omega} \sin Q \\ \frac{1}{2\omega}(\alpha^2 - \beta^2) \sin Q & \frac{i(\beta^2 - \sigma^2)}{2\omega} \cos Q \end{pmatrix} \tag{12}$$

For interface 2 we write a similar equation:

$$\begin{pmatrix} v_{x_2} \\ v_{z_2} \\ z_{z_2} \\ \frac{1}{2\mu} z_{x_2} \end{pmatrix} = B \begin{pmatrix} \phi' + \phi'' \\ \phi' - \phi'' \\ \Psi' - \Psi'' \\ \Psi' - \Psi'' \end{pmatrix} \tag{13}$$

where B is obtained from A by letting $P - Q = 0$. Of more interest is the inverse of B:

$$B^{-1} = \begin{pmatrix} \frac{-2i\sigma}{K^2} & 0 & \frac{i\omega}{\mu K^2} & 0 \\ 0 & \frac{-i(-\sigma^2+\beta^2)}{\alpha K^2} & 0 & \frac{2i\sigma\omega}{\alpha K^2} \\ \frac{i(\lambda k + 2\alpha^2\mu)}{\beta\mu K^2} & 0 & \frac{i\sigma\omega}{\beta\mu K^2} & 0 \\ 0 & -2i\sigma/K^2 & 0 & \frac{-2i\omega}{K^2} \end{pmatrix} \tag{14}$$

We are using the notation of Brekhovskikh[7] and Spielvogel.[8] We take

$$k^2 = \sigma^2 + \alpha^2 \tag{15}$$

$$K^2 = \sigma^2 + \beta^2 \tag{16}$$

and use

$$\mu K^2 = k^2(2\mu + \lambda) \tag{17}$$

from Eqs. 5 and 6.

Combining Eqs. 11 and 13 we have

$$\begin{pmatrix} v_{x1} \\ v_{z1} \\ z_{z1} \\ \frac{1}{2\mu} z_{x1} \end{pmatrix} = AB^{-1} * \begin{pmatrix} v_{x2} \\ v_{z2} \\ z_{z2} \\ \frac{1}{2\mu} z_{z2} \end{pmatrix} = a^* \begin{pmatrix} v_{x2} \\ v_{z2} \\ z_{z2} \\ \frac{1}{2\mu} z_{x2} \end{pmatrix} \tag{18}$$

we let $\sin\theta = \sigma/k$ and $\sin\gamma = \sigma/k$ so the components of a are

$$a_{11} = 2\sin^2\gamma\cos P + \cos 2\gamma\cos Q \tag{19}$$

$$a_{12} = i(\tan\theta\cos 2\gamma\sin P - \sin 2\gamma\sin Q) \tag{20}$$

$$a_{13} = \frac{\sin\theta}{\rho c}(\cos Q - \cos P) \tag{21}$$

$$a_{14} = -2ib(\tan\theta\sin\gamma\sin P + \sin Q\cos\gamma) \tag{22}$$

$$a_{21} = i\left[\frac{b \cos\theta \sin 2\gamma \sin P}{c \cos\gamma} - \tan\gamma \cos 2\gamma \sin Q\right] \tag{23}$$

$$a_{22} = \cos 2\gamma \cos P + 2 \sin^2\gamma \cos Q \tag{24}$$

$$a_{23} = \frac{-i}{\rho c}(\cos\theta \sin P + \tan\gamma \sin\theta \sin Q) \tag{25}$$

$$a_{24} = 2b \sin\gamma (\cos Q - \cos P) \tag{26}$$

$$a_{31} = 2\rho b \sin\gamma \cos 2\gamma (\cos Q - \cos P) \tag{27}$$

$$a_{32} = -i\rho\left(c\frac{\cos^2 2\gamma}{\cos\theta}\sin P + 4b \cos\gamma \sin^2\gamma \sin Q\right) \tag{28}$$

$$a_{33} = \cos 2\gamma \cos P + 2 \sin^2\gamma \cos Q \tag{29}$$

$$a_{34} = 2i\rho b^2 (\cos 2\gamma \tan\theta \sin P - \sin 2\gamma \sin Q) \tag{30}$$

$$a_{41} = -i\left(\frac{2}{c}\cos\theta \sin^2\gamma \sin P + \frac{\cos^2 2\gamma \sin Q}{2b \cos\gamma}\right) \tag{31}$$

$$a_{42} = \frac{\sin\theta \cos 2\gamma}{c}(\cos Q - \cos P) \tag{32}$$

$$a_{43} = \frac{i}{2\rho}\left(\frac{\sin 2\theta \sin P}{c^2} - \frac{\cos 2\gamma \tan\gamma \sin Q}{b^2}\right) \tag{33}$$

$$a_{44} = 2 \sin^2\gamma \cos P + \cos 2\gamma \cos Q \tag{34}$$

The last component of Eq. 18 is

$$\frac{1}{2\mu} z_{x1} = a_{41} v_{x2} + a_{42} v_{z2} + a_{43} z_{z2} + a_{44} z_{x2}/2\mu \tag{35}$$

This equation describes what happens at the glass fluid interface. However, since there can be no transverse stress in the fluid we must also have no transverse stress in the glass at the boundary: $z_{x1} = z_{x2} = 0$. Therefore Eq. 35 reduces to

$$a_{41} v_{x2} + a_{42} v_{z2} + a_{43} z_{z2} = 0 \tag{36}$$

Incorporating Eq. 36 into Eq. 18 we obtain

$$v_{x1} = \left(a_{12} - \frac{a_{11}a_{42}}{a_{41}}\right) v_{z2} + \left(a_{13} - \frac{a_{11}a_{43}}{a_{41}}\right) z_{z2} \tag{37}$$

$$\begin{pmatrix} v_{z1} \\ z_{z1} \end{pmatrix} = \begin{pmatrix} M_1 & M_2 \\ M_3 & M_4 \end{pmatrix} \begin{pmatrix} v_{z2} \\ z_{z2} \end{pmatrix} \tag{38}$$

where

$$M_1 = a_{22} - a_{21}a_{42}/a_{41} \tag{39}$$

$$M_2 = a_{23} - a_{21}a_{43}/a_{41} \tag{40}$$

$$M_3 = a_{32} - a_{31}a_{42}/a_{41} \tag{41}$$

$$M_4 = a_{33} - a_{31}a_{43}/a_{41} \tag{42}$$

In a fluid $b = 0$ and $\gamma = 0$ so to relate v_z and z_z between interfaces 2 and 3 we have analogous to Eq. 38:

$$\begin{pmatrix} v_{z2} \\ z_{z2} \end{pmatrix} = \begin{pmatrix} a_{22}' & a_{23}' \\ a_{32}' & a_{33}' \end{pmatrix} \begin{pmatrix} v_{z3} \\ z_{z3} \end{pmatrix} \tag{43}$$

where

$$a_{22}' = \cos P_{LC} \tag{44}$$

$$a_{23}' = \frac{-i \sin P_{LC} \cos \theta_{LC}}{\rho_{LC} C_{LC}} \tag{45}$$

$$a_{32}' = \frac{-i\rho_{LC} C_{LC} \sin P_{LC}}{\cos \theta_{LC}} \tag{46}$$

$$a_{33}' = \cos P_{LC}, \tag{47}$$

where the LC subscript refers to the value of these parameters in the liquid crystal region.

We have for the second glass region:

$$\begin{pmatrix} v_{z3} \\ z_{z3} \end{pmatrix} = \begin{pmatrix} M_1 & M_2 \\ M_3 & M_4 \end{pmatrix} \begin{pmatrix} v_{z4} \\ z_{z4} \end{pmatrix} \tag{48}$$

where the M_i's are given in Eqs. 39–42. Eqs. 38, 43, and 48 combine to give

$$\begin{pmatrix} v_{z1} \\ z_{z1} \end{pmatrix} = \begin{pmatrix} C_1 & C_2 \\ C_3 & C_4 \end{pmatrix} \begin{pmatrix} v_{z4} \\ z_{z4} \end{pmatrix} \tag{49}$$

where

$$\begin{pmatrix} C_1 & C_2 \\ C_3 & C_4 \end{pmatrix} = \begin{pmatrix} M_1 & M_2 \\ M_3 & M_4 \end{pmatrix} \begin{pmatrix} a_{22}' & a_{23}' \\ a_{32}' & a_{33}' \end{pmatrix} \begin{pmatrix} M_1 & M_2 \\ M_3 & M_4 \end{pmatrix} \tag{50}$$

Equation 49 relates the z component of stress and velocity of interface 1, the first interface the incident wave encounters, to interface 4, the final interface of the cell. We may now match the incident wave with interface 1 and the transmitted wave with interface 4 and thereby find the acoustic transmission of the cell. We will change the origin of the coordinate system in Figure 1 so it lies in

interface 4 and take the complete cell thickness from 1 to 4 to be H. Then for the initial wave we have

$$\phi_a = [\phi'_a e^{i\alpha_a(z-H)} + \phi''_a e^{-i\alpha_a(z-H)}]e^{-i(\sigma_a x-\omega t)} \tag{51}$$

$$\Psi_a = 0 \tag{52}$$

where ϕ'' is the amplitude of the incident wave and ϕ' the amplitude of the reflected wave. The wave is traveling in the negative z direction.

Similarly for fluid b

$$\phi_b = \phi''_b e^{-i\alpha_b z} e^{i(\sigma_a x-\omega t)} \tag{53}$$

for the wave transmitted through the cell. Using Eqs. 3, 4, and 7–10 and omitting the common factor of $e^{i(\alpha x-\omega t)}$ we have

$$v_{xa} = i\sigma_a(\phi'_a + \phi''_a) \tag{54}$$

$$v_{za} = i\alpha_a(\phi'_a - \phi''_a) \tag{55}$$

$$z_{xa} = 0 \tag{56}$$

$$z_{za} = -i\omega\rho_a(\phi'_a + \phi''_a) \tag{57}$$

$$v_{xb} = i\sigma_b\phi''_b \tag{58}$$

$$v_{zb} = i\alpha_b\phi''_b \tag{59}$$

$$z_{zb} = i\omega\rho_b\phi''_b \tag{60}$$

From Eq. 49 we have

$$\begin{pmatrix} -\alpha_a(\phi'_a - \phi''_a) \\ \omega\rho_a(\phi'_a + \phi''_a) \end{pmatrix} = \begin{pmatrix} C_1 & C_2 \\ C_3 & C_4 \end{pmatrix} * \begin{pmatrix} \alpha_b & \phi''_b \\ \omega\rho_b & \phi''_b \end{pmatrix} \tag{61}$$

We define the transmission coefficient as

$$D = \rho_b\phi''_b/\rho_a\phi''_a \tag{62}$$

and the reflection coefficient as

$$V = \phi'_a/\phi''_a \tag{63}$$

Equation 61 provides the means by which these coefficients may be evaluated. To calculate the transmitted acoustic intensity we must evaluate $|D|$. Care must be taken in doing so, however. The longitudinal speed in the glass is over three times the speed in the water. Use of Snell's law shows the critical angle for the two types of glass we use occurs at 15 degrees and 15.5 degrees. Similarly, the shear wave speed in the glass is over twice the longitudinal speed in the water. For the two types of glass we use the critical angle for this type of wave is exceeded at 25.5 and 27 degrees. Therefore, we find three regions for the angle of incidence. A separate equation for the transmission must be found

for each region: the region where no critical angle is exceeded, where only the critical angle for the longitudinal wave is exceeded and where both critical angles are exceeded. For example, in the second region taking θ to be the angle for the compression wave in the glass and θ_a in the water we have from Snell's law

$$\sin\theta = \frac{C\sin\theta_a}{C_a} \qquad \text{so if } \frac{C\sin\theta_a}{C_a} > 1 \text{ then}$$

$$\cos\theta \to i\sqrt{\sin^2\theta - 1} \tag{64}$$

$$\sin P \to i\sin h\,|P| \tag{65}$$

$$\cos P \to \cos h\,|P| \tag{66}$$

Similarly, if both critical angles are exceeded we must make changes in $\cos\gamma$, $\sin Q$, and $\cos Q$.

Therefore, certain terms which are real in the matrices for one region will be imaginary in another. Nevertheless we do find for all regions:

$$|D|^2 = \frac{4\omega^2\rho_b^2/\alpha_b^2}{\left[\frac{\omega\rho_b}{\alpha_b}|C_4| + \frac{\omega\rho_a|C_1|}{\alpha_a}\right]^2 + \left[|C_3| + \frac{\omega^2\rho_a\rho_b|C_2|}{\alpha_a\alpha_b}\right]^2} \tag{67}$$

although the form for $|C_i|$ will change for each region.

Equation 67 will be the basis of comparison for the measurements we will make for the amount of ultrasound transmitted through the liquid crystal cell. It should be noted that Eq. 67 does not include any damping due to either viscosity or surface waves in the cell. Furthermore, we have omitted the small anisotropy for the speed of sound which occurs in liquid crystals. The latter simplification appears to be less severe than the former ones.

III EXPERIMENT

A Single layer verification

To test Eq. 67 experimentally, we start with the simple case of a single sheet of glass rather than the liquid crystal cell mentioned above. For this case the $|C_i|$ reduce to the $|M_i|$ of Eqs. 39–42.

Two Panametrics Model V302 transducers are used for the transmitter and hydrophone. The transmitter is driven by a Hewlett-Packard Model 3312A function generator in the amplitude modulation mode externally modulated by a Hewlett-Packard Model 3310A pulse generator. Pulses were typically 25 μ sec in width containing approximately 20 cycles per pulse. The frequency is measured using a Hewlett-Packard Model 5326A timer/counter. The glass sheet is placed in the center of a water tank 30 cm $\times$ 40 cm $\times$ 60 cm. The

acoustic transmitter is located 8 cm from the glass sheet with the hydrophone approximately the same distance on the other side. The glass is suspended by an angular positioning device allowing orientation to the nearest degree to be specified. Initial alignment is facilitated by a laser. The signal from the hydrophone is amplified and sent to both a PAR Model 160 boxcar integrator and Tektronix 564 oscilloscope. For the data on the graphs presented in this section the values are read from the oscilloscope.

The glass sheets are 15 cm × 15 cm × 0.16 cm and 15 cm × 15 cm × 0.0146 cm, respectively. The diameter of both the transmitter and hydrophone are 2.5 cm. By noting the time of the various pulses displayed on the oscilloscope the reflection source may be identified. As the orientation of the glass changes the times between the reflection pulses and main pulse changes. The largest reflected pulse amounts to 10% of the main pulse.

The following constants are used for the thicker glass, longitudinal and shear speeds: 5.61×10^5 cm/sec and 3.32×10^5 cm/sec, respectively, with a density of 2.54 gm/cm^3. For the thin glass these values are 5.81×10^5 cm/sec,

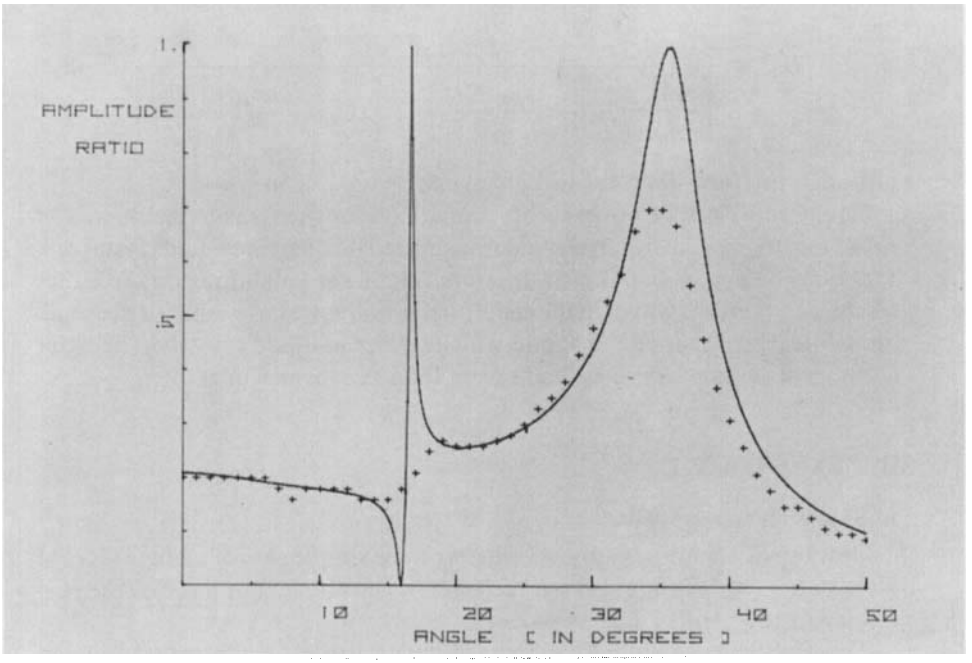

FIGURE 2 A graph of the ratio of voltages from the hydrophone with and without a single sheet of 1.6 mm thick glass as a function of angle. Therefore, this graph shows the acoustic transmission of the glass as a function of angle. The crosses are experimental points. The solid line is from Eq. 67 for $|D|$. Since each factor in the equation is measured there are no adjustable parameters used to induce the fit. Therefore, the graph represents a severe testing of the theory. For this graph the thicker glass cell is used and a frequency of 0.858 MHz. No correction is made for the finite acceptance angle of the hydrophone.

3.48×10^5 cm/sec and 2.51 gm/cm^3, respectively. The thicker glass is float glass obtained from PPG Industries. The manufacturer supplied the values of Young's modulus, 1.0×10^7 lb/in^2, and the Poisson ratio, 0.23, from which the above acoustic speeds are obtained. The thin glass is obtained from Corning Glass Co. which supplied the shear modulus, 4.4×10^6 psi, and Poisson ratio, 0.22, from which the acoustic speeds for the thin glass are calculated.

Figure 2 is a graph of the ratio of the hydrophone voltage with the glass present to that without. The abscissa is the angle between the normal to the glass plate and that of the acoustic beam. The crosses are the experimental values obtained approximately every degree. The solid line is the theoretical result from Eq. 67 for $|D|$ using the above constants.

It should be noted that there are no adjustable parameters used in this graph since each constant of Eq. 67 is known. There are two peaks of 100% transmission in the theoretical plot at 16.5 degrees and at 35.4 degrees, as well as a dip to zero transmission at 15.9 degrees. Experimentally the crosses in the graph show the upper peak, though shifted to 34.5 degrees and reduced from 100% to 70% transmission. The lower peak and dip are missing, however. These discrepancies are due in part to the finite acceptance angle of the hydrophone. Figure 3 is identical to Figure 2 except each point on the theoretical plot is

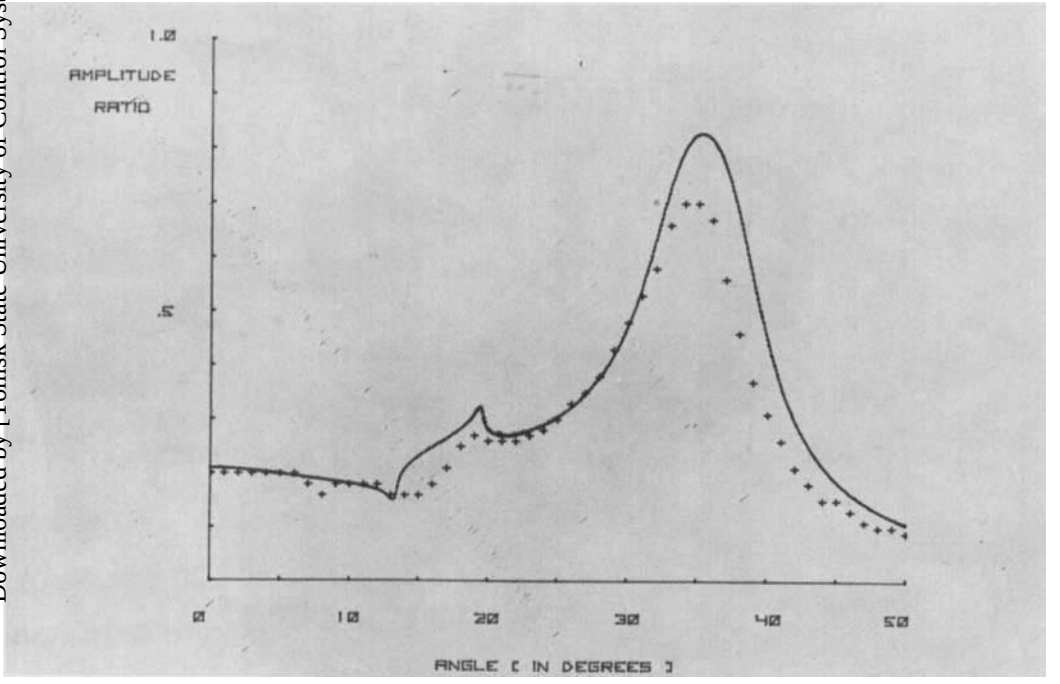

FIGURE 3 Identical to Figure 2 only correction is made for the finite acceptance angle of the hydrophone.

averaged over the values for 3 degrees on each side. The averaging brings the upper peak down to a maximum of 82.9% and places it at 35.2 degrees as well as greatly reducing the lower peak and almost eliminating the dip. This averaging will be performed in the subsequent graphs.

Figure 4 shows the comparison of theory and experiment for a single sheet of the thin glass. The theory appears to uniformly predict two to three percent higher transmission than what is realized experimentally, in agreement with Figure 3. Considering we have omitted any dissipation of the sound wave we would expect such a result. A frequency of 0.858 MHz is used for Figures 2 and 3 and 0.857 MHz for Figure 4. For the thicker glass the resulting wavelengths for the longitudinal and shear waves are, respectively, 0.65 cm and 0.39 cm. The ratio of wavelength to glass thickness is 0.25 and 0.41, respectively. For the thinner glass the longitudinal and shear wavelengths are 0.021 and 0.036, respectively. It is this smaller ratio for the thin glass which makes it suited for the nematic cell exhibiting the acousto-optic effect. We shall see the uniform higher sound transmission allows for a greater light transmission in the acousto-optic effect with less angular sensitivity.

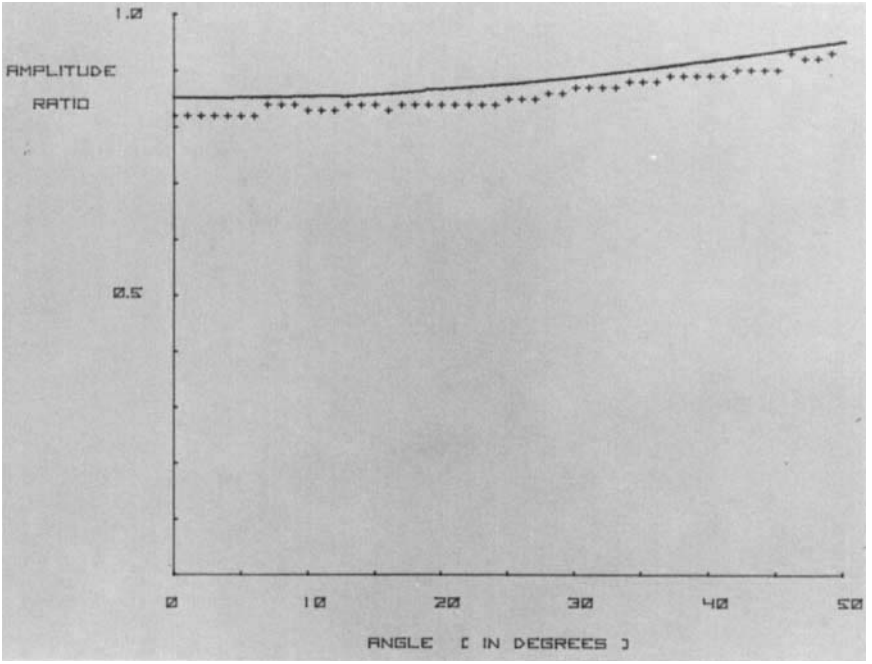

FIGURE 4 A graph of the ratio of voltages from the hydrophone with and without a single sheet of 0.146 mm thick glass as a function of angle. The frequency is 0.857 MHz.

B Liquid crystal cell investigation

The nematic liquid crystal is 4-cyano-4'-*n* hexyl biphenyl commonly known as K18. The transition temperature for the crystal to nematic phase transition occurs at 14.5°C and the nematic to isotropic transition at 20.4°C. It is obtained from Atomergic Chemetals Corp. and used without further purification.

Each cell is constructed by coating two glass sheets with lecithin to promote homeotropic alignment of the liquid crystal. The coated sides are placed next to one another with 80 μm spacers at the edges. The liquid crystal is then introduced at the glass edges between the spacers and pulled into the cell by capillary action.

After the cell has been filled with the nematic the edges are coated with wax. Epoxy is then applied at all edges. The wax is used to prevent the nematic from reacting chemically with the epoxy. For cells made with the thin glass the cell is mounted in a plexiglass frame for added support.

The acoustic wave for these cells is generated by the method described above or with a Medi Sonar Model 1100 ultrasonic generator. The latter operates at 1 MHz and is used when greater power is required. Intensities of 1.1 Watts/cm^2 may be obtained with this unit.

For measurement of the light transmitted by the acousto-optic effect a 150 Watt lamp is used. Light passes through the liquid crystal cell, a second polarizer with an axis oriented at 90 degrees to the first, and to a photomultiplier. The signal from the photomultiplier is amplified and sent to a digital voltmeter.

Figure 5 shows the ratio of voltage of the hydrophone, with and without the liquid crystal cell, as a function of angle. For Figure 5 the cell is constructed of the thicker glass and an acoustic frequency of 1 MHz is used. The crosses are the experimental ratios and the solid line is the theoretical value of the absolute value of D from Eq. 67. The solid points on the graph are for the light intensity in arbitrary units transmitted via the acousto-optic effect.

It would appear the acousto-optic effect is operative when the cell configuration allows maximum transmission of sound. This result appears to explain the results of Letcher, Lebrun and Candau[2] who reported a strong optical signal for only a narrow range of incident angles, 27 to 30 degrees. This result is also in agreement with Nagai, Peters and Candau[3] who found a correlation with experimental acoustic and optical transmission. Equation 67 also explains their results for acoustic transmission versus film thickness, their Figure 7. Also, the broadening of the transmission for thin glass as reported by Lebrun, Candau and Letcher[2] is explained. This result is in disagreement with that of Perbet, Hareng and LeBerre[5] who report an optical signal for large acoustic reflection. We find no optical signal for large acoustic reflection.

If we conclude that Eq. 67 may be used to predict maximum acoustic transmission and therefore maximum transmitted light from the acousto-optic ef-

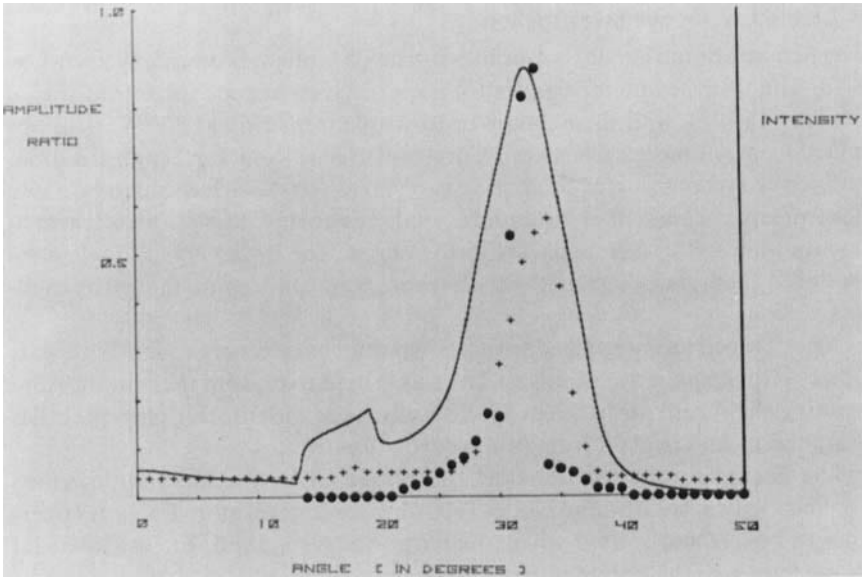

FIGURE 5 A graph of acoustic transmission through a liquid crystal cell made of the 1.6 mm thick glass as a function of incident acoustic angle. The acoustic transmission is measured as the ratio of voltage from the hydrophone with and without the presence of the liquid crystal cell. The solid line is the theoretical value of $|D|$ from Eq. 67. The crosses are the measured values of acoustic transmission. The filled circles are measured values of transmitted light intensity via the acousto-optic effect using arbitrary linear units. It should be noted that the maximum light intensity occurs at the incident angle for maximum acoustic transmission.

fect it would appear the equation could be used to prescribe how a given cell should be made for a particular acoustic frequency. Or if the cell size is determined by other considerations, Eq. 67 could be used to prescribe the acoustic frequency which should be used. For instance, for the thicker glass cell used in Figure 5, assuming an incident angle of zero, Eq. 67 is used to determine the acoustic transmission. See Figure 6. The results indicate that an acoustic frequency of around 500 kHz would give the best results.

For Figure 7 the cell was constructed of the thinner glass sheets. Again we see as the acoustic transmission increases more light is transmitted. In comparing Figure 7 with Figure 4 and Figure 5 with Figure 3 we see the difference in the theoretical sound transmission and experimental sound transmission increases as one changes from a single glass sheet to a liquid crystal cell. The increase is reasonable since the means of dissipation has increased. The flows induced in the liquid crystal which give rise to the acousto-optic effect are in fact an added means of dissipation of the acoustic energy.

Another means of dissipation is the surface wave generated. Figure 8 shows a series of photographs for the cell viewed between crossed polarizes. The photographs labeled A to F have the incident acoustic beam at angles 0°, 4°, 12.5°,

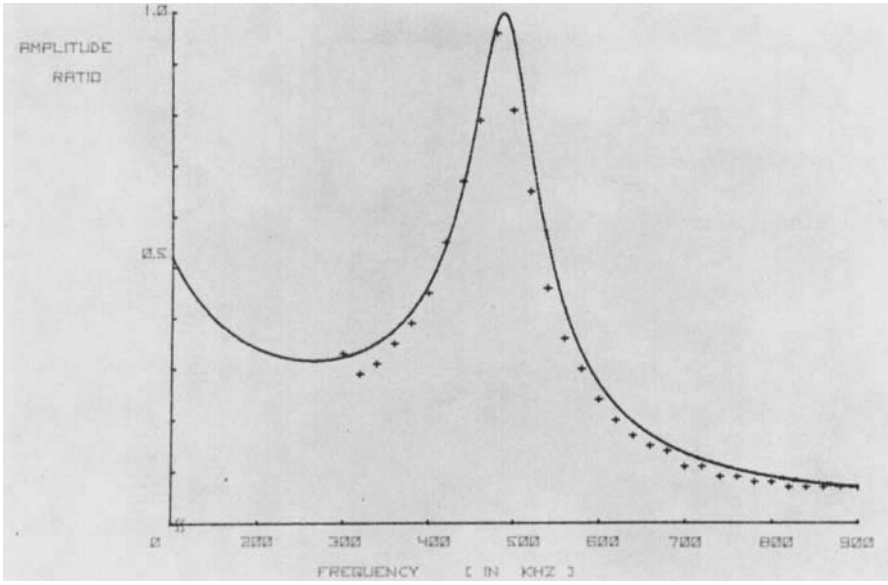

FIGURE 6 A graph of acoustic transmission as a function of acoustic frequency. The solid line is the theoretical value from Eq. 67. The crosses are the experimental values. There are no adjustable parameters used to induce the fit since each parameter in Eq. 67 is known or measured. A liquid crystal cell made of 1.6 mm thick glass is used for these results.

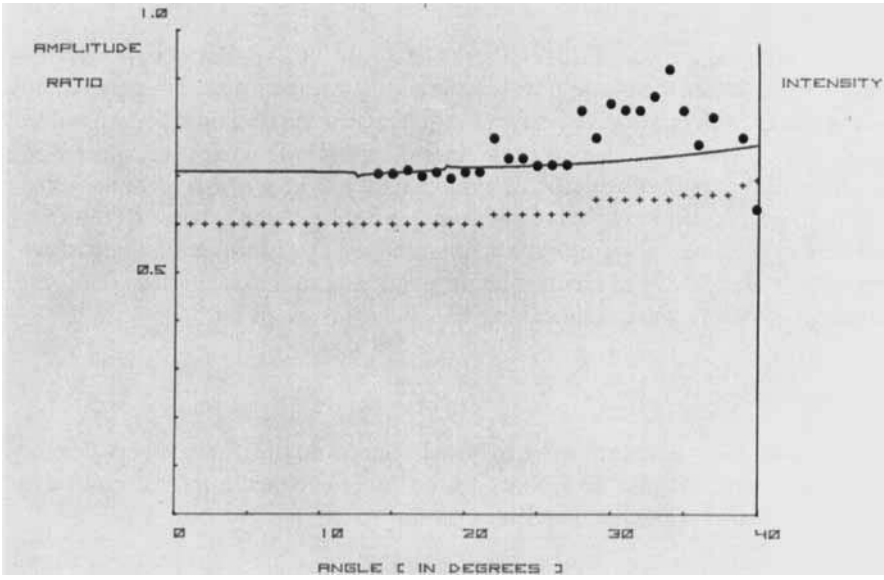

FIGURE 7 Similar to Figure 5 only the liquid crystal cell is constructed of thinner glass, 0.146 mm thick. The filled circles represent measured values of transmitted light intensity via the acousto-optic effect.

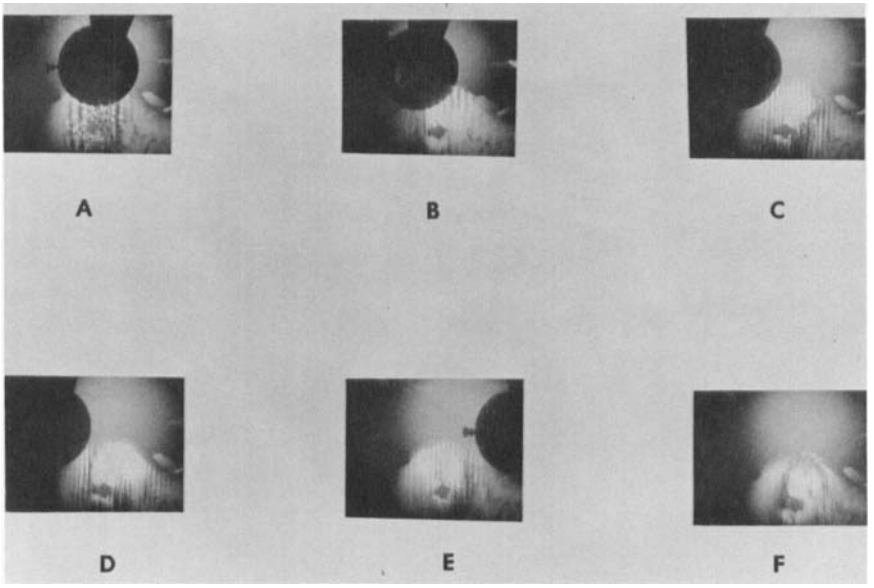

FIGURE 8 A series of pictures of the liquid crystal while excited by an ultrasonic wave. The spacing between the resulting vertical lines is seen to decrease with increasing acoustic angle. The angle of incidence for each picture is: A. zero degrees B. four degrees C. twelve and one half degrees D. fifteen degrees E. negative seventeen degrees (from the right rather than left) F. thirty three degrees

15°, −17° (from the right rather than the left), and 33°. The dark circle with the knob on the left in the photographs is the acoustic transmitter. The small tilted rectangle in each picture is a spacer. In each picture vertical lines are shown. In the absence of acoustic waves these lines disappear. The light transmitted in each line is the result of acoustic streaming in the liquid crystal (i.e. the acousto-optic effect). As the angle of incidence increases the distance between the lines decreases. Figure 9 is a graph of the line spacing as a function of angle. If we imagine a plane wave of incident angle, θ, coming to the cell surface the component, d, of the wavelength along the surface is given by

$$d = \frac{\lambda}{\sin \theta} \tag{68}$$

We would expect a surface wave to be generated and the distance between the lines to be proportional to d. Since for normal incidence Eq. (68) shows d to become infinite we generalize the equation to

$$\text{line space} = a/\sin(\theta + b) \tag{69}$$

where a and b are constants. The constant b should result from the divergence of the incident acoustic beam. The continuous curve in Figure 9 is for Eq. 69 with $a = 1.25$ mm and $b = 14.38$ degrees. Lines similar to these have been re-

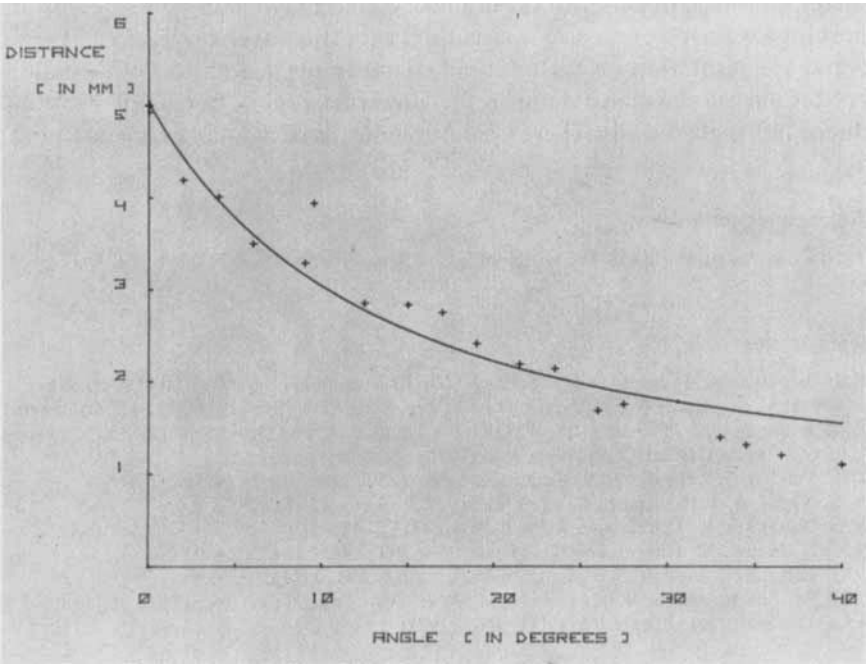

FIGURE 9 A graph of the distance between the lines such as those shown in Figure 8 as a function of incident angle. The solid line is the fit from Eq. 69.

ported by Perbet, Hareng, and LeBerre.[5] The angular dependence we observe lends support to their claim that the lines result from surface waves.

IV CONCLUSIONS

We have developed an equation to allow evaluation of the acoustic transmission through a liquid crystal cell as a function of incident acoustic angle, frequency and thickness, density and acoustic speeds of the materials in the cell. Although a number of simplifying assumptions are made in the derivation, such as omitting viscous dissipation, we find good agreement between the theoretical prediction and the experimental realization for acoustic transmission. We also find a positive correlation between the maximum acoustic transmission and the maximum sensitivity for the acousto-optic effect. Therefore, the transmission equation may be used to prescribe cell structure and acoustic frequency for the utilization of the acousto-optic effect. The maximum acoustic transmission of the cell occurs at those angles where the component of the incident wavelength along the glass surface matches the wavelength of a flexural or peristaltic wave along the glass at the imposed acoustic frequency. Therefore, the maximum acoustic transmission occurs when the liquid crystal boundaries have their largest amplitudes of oscillation and

therefore when streaming of the liquid crystal is maximum. This result is important for the resolution of a visualized acoustic wavefront pattern. To increase the resolution we must not only dampen the lateral flow of the liquid crystal but we must also dampen the lateral flexural or peristaltic wave induced in the glass walls. There are several means of inducing such damping.

Acknowledgment

This work was supported by the Office of Naval Research, Contract N00014-78-C-0417.

References

1. C. Sripaipan, C. F. Hayes and G. T. Fang, Sixth International Liquid Crystal Conference, J-29 (1976). C. Sripaipan, C. F. Hayes and G. T. Fang, *Phys. Rev.*, **15A**, 1297 (1977). K. Miyano and Y. R. Shen, *Appl. Phys. Lett.*, **28**, 473 (1976). S. Candau, A. Peters and S. Nagai, Sixth International Liquid Crystal Conference, J-30 (1976).
2. S. Letcher, J. Lebrun and S. Candau, *J. Acoust. Soc. Am.*, **63**, 55 (1978).
3. S. Nagai, A. Peters and S. Candau, *Revue Phys. Appl.*, **12**, 21 (1977).
4. S. Nagai and K. Iizuka, *Jpn. J. Appl. Phys.*, **17**, 723 (1978).
5. J. N. Perbet, M. Hareng and S. LeBerre, *Rev. Phys. Appl.*, **14**, 569 (1979).
6. J. Lebrun, S. Candau, S. V. Letcher, *J. Phys.*, **C3**, 298 (1979).
7. L. M. Brekhovskikh, *Waves in Layered Media* (Academic, New York, 1960), pp. 56 ff.
8. L. Q. Spielvogel, *J. Appl. Phys.*, **42**, 3667 (1971).